The evolution of activity in galaxies from z=0.45 to the present time

Grażyna Stasińska[1], M. V. Costa-Duarte[1,2] and N. Vale Asari[3]

[1]LUTH, Observatoire de Paris, CNRS, Université Paris Diderot,
Place Jules Janssen, F-92190 Meudon
email: `grazyna.stasinska@obspm.fr`

[2]Instituto de Astronomia, Geofísica e Ciências Atmosféricas, Universidade de São Paulo,
São Paulo, Brazil
email: `mvcduarte@astro.iag.usp.br`

[3]Departamento de Física - CFM - Universidade Federal de Santa Catarina,
Florianópolis, SC, Brazil
email: `natalia@astro.ufsc.br`

Abstract. We use spectra from the SDSS to study the signatures of nuclear activity over cosmic time, dividing the samples in redshift and mass bins, and using various diagnostic diagrams. A redshift evolution clearly emerges from the analysis of our diagrams.

Keywords. surveys, galaxies: general, galaxies: active

1. Introduction

Studying the interplay between star forming, AGN and passive phases of galaxy evolution requires:
- A wide database of adequate galaxy spectra.
- Properly defined criteria for these different phases of galaxy evolution.
- Binning the sample into stellar mass ($M_\star$) and redshift (z) bins to adequately deal with the problem of downsizing (Cowie *et al.* 1996) and completeness.

2. The binned SDSS/DR7 galaxy sample

- We extracted our database from the Sloan Digital Sky Survey (SDSS/DR7, Abazajian *et al.* 2009) main galaxy sample, applying the following restrictions: redshift > 0.002 and z-band aperture covering factor > 20% (to reduce aperture effects and avoid intragalactic sources). Additional restrictions were applied depending on the considered properties (see below)
- The current total stellar mass $M_\star$ and the measurements of the Hα, [NII]6584, [OIII]5007 and Hβ emission lines were taken from the STARLIGHT database (http://casjobs.starlight.ufsc.br/casjobs/).
- The database was divided in $M_\star$ bins of 0.5 dex between $9 < \log M_\star / M_\odot < 12$ and in z bins of 0.05 from 0.05 to 0.45. Bins corresponding $\log M_\star$ $M_\odot < 9$ and $\log M_\star$ $M_\odot > 12$ are also shown but they cover a wider range of stellar masses.
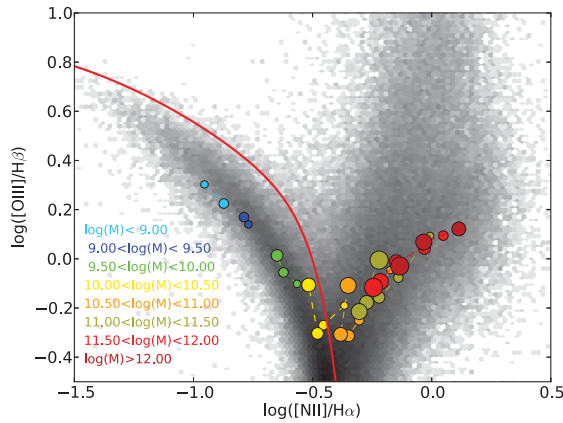
Figure 1. The BPT diagram for galaxies that have a signal-to-noise ratio of at least 3 in the four relevant lines. Circles show the position of the average values of $[OIII]/H\beta$ vs $[NII]/H\alpha$ for each $(M_\star, z)$ bin. Larger circles represent higher redshifts. Different colours represent different $M_\star$ bins, blue for the smallest $M_\star$ and red for the largest ones. The curve represents the S06 divisory line. The background density map represents the entire SDSS/DR7 galaxy sample from $0.05 < z < 0.1$.

3. The BPT and WHAN diagrams

3.1. *The BPT diagram*

To distinguish between SF galaxies and AGN hosts, the $[OIII]/H\beta$ versus $[NII]/H\alpha$ diagram (Baldwin *et al.* 1981, BPT) is generally used. Since the study by Kauffmann *et al.* (2003, K03) it is common practise to consider galaxies as star-forming when they lie below the empirical K03 line, AGN hosts when they lie above the "extreme starburst line" of Kewley *et al.* (2001, K01) line, and "composite" when they are found in-between. However Stasińska *et al.* (2006, S06) and Dopita *et al.* (2013) have produced a more appropriate theoretical line to separate *pure* SF galaxies from the rest.

- When plotting the average values of $[OIII]/H\beta$ versus $[NII]/H\alpha$ it appears that the 3 lowest $M_\star$ bins are all entirely in the pure SF region and that the metallicity of the interstellar medium (as indicated by $[NII]/H\alpha$) increases with time.
- The higher $M_\star$ bins are located in the right wing. Taking the BPT diagram as a perfect diagnostic for the presence of AGNs, one would erroneously infer that the importance of AGN versus star formation increases with time for these $M_\star$ bins, since the points tend to go to the right as redshift decreases.

3.2. *The WHAN diagram*

However, as shown by Stasińska *et al.* (2008) and further discussed by Cid Fernandes *et al.* (2011), retired galaxies (i.e., emission-line galaxies that have stopped forming stars and are ionized by hot low-mass evolved stars – HOLMES) have the same location in the BPT diagram as galaxies hosting weak AGNs.

- The WHAN diagram (Cid Fernandes *et al.* 2011) allows one to distinguish between pure SF galaxies, AGN hosts (strong and weak) and passive galaxies (i.e. retired galaxies and lineless galaxies).
- The highest $M_\star$ bins clearly enter the region of passive galaxies as redshift decreases.
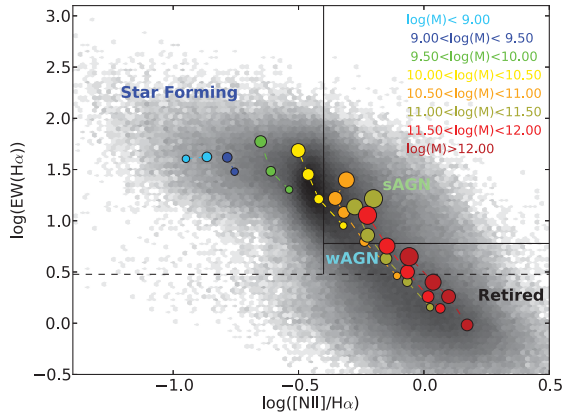
Figure 2. The WHAN diagram. The circles represent the position of the average values of EW(Hα) versus [NII]/Hα for each $(M_\star, z)$ bin in our database, excluding those galaxies whose spectra have "bad" pixels in the Hα or [NII] region.
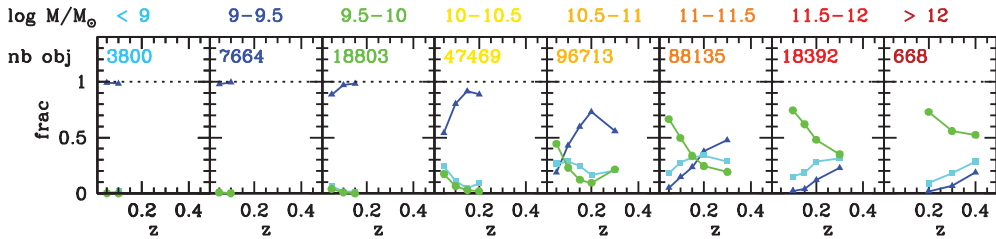
Figure 3. Fraction of galaxies of different spectral types as a function of redshift for the different mass bins as obtained from the canonical use of the BPT diagram using the K01 and K03 divisory lines. Blue triangles: SF; green circles: AGN, and cyan squares: composite.

## 4. A detailed census of galaxy types in $(M_\star, z)$ bins

While discussing how *average* properties of galaxies change with $M_\star$ or z, one must nor forget to also examine their *dispersion*. In the $(M_\star, z)$ bins, some galaxies can be pure SF ones, while others may contain an AGN, and many of them may have no emission lines at all.

4.1. *According to the classical use of the BPT diagram*

• Low $M_\star$ bins present a predominance of SF galaxies. As $M_\star$ increases the presence of an AGN host becomes more common and becomes dominant at the highest $M_\star$.

• In the highest $M_\star$ bins "composite" galaxies behave similarly to SF galaxies, while they behave similarly to AGN galaxies for log $M_\star / M_\odot < 11$.

• The proportion of SF galaxies decreases as redshift decreases while that of AGN hosts increases with decreasing redshift. For log $M_\star\ M_\odot < 10.5$ the population of galaxies entering the BPT diagram and classified in the canonical way as SF largely dominates at any redshift.

4.2. *According to the WHAN diagram*

The WHAN diagram allows one to distinguish between weak AGNs and retired galaxies (erroneously counted as AGN hosts or "composite" when using the BPT diagram in a classical way). This permits a true census of galaxies of various spectral types in the local Universe. Note that, like Cid Fernandes *et al.* (2011) we distinguish between *pure* SF
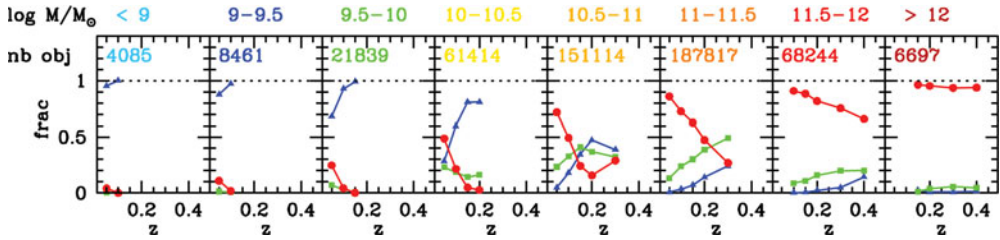
Figure 4. Fraction of SF galaxies (blue triangles), AGN hosts (green squares) and passive – retired and lineless – galaxies (red circles) found from the WHAN diagram as a function of z.

galaxies and galaxies showing at least a trace of an AGN contribution (so our definition of SF objects is not identical to that of Kauffmann *et al.* 2003). We see that:

• Low $M_\star$ bins present a predominance of SF galaxies while high $M_\star$ bins present a predominance of passive galaxies. AGN hosts never represent the dominant fraction if all galaxies are taken together.

• The fraction of passive galaxies increases with decreasing z indicating a decrease of star formation with time. The highest $M_\star$ bins, however, are almost entirely populated by passive galaxies at all the sampled redhifts, indicating that the bulk of star formation in them occured over 4 Gyr ago (corresponding to $z = 0.4$).

5. Summary and conclusions

• Because of downsizing, the study of the evolution of SF galaxies and AGN hosts needs to be done in stellar mass bins.

• Retired galaxies cannot be distinguished from weak AGNs (LINER-type galaxies) in the BPT diagram. Differentiation can be done using the WHAN diagram.

• Studies dealing with the redshift evolution of galaxies cannot ignore the existence of lineless galaxies, and thus cannot be based on emission-line diagnostics only.

• The BPT and WHAN diagram lead to very different views of the evolution of galaxy spectral types in the local Universe.

References

Abazajian, K. N., *et al.*, 2009, *ApJS*, 182, 543

Baldwin, J. A., Phillips, M. M., & Terlevich, R., 1981, *PASP*, 93, 5

Cid Fernandes, R., Stasińska, G., Mateus, A., & Vale Asari, N., 2011, *MNRAS*, 413, 1687

Cowie, L. L., Songaila, A., Hu, E. M., & Cohen, J. G., 1996, *AJ*, 112, 839

Dopita, M. A., *et al.* , 2013, *ApJS*, 208, 10

Kauffmann, G., *et al.*, 2003, *MNRAS*, 346, 1055

Kewley, L. J., Dopita, M. A., Sutherland, R. S., Heisler, C. A., & Trevena, J., 2001, *ApJ*, 556, 121

Stasińska, G., *et al.*, 2008, *MNRAS*, 391, L29